A green organic-solvent-free route to prepare nanostructured zinc oxide carriers of clotrimazole for pharmaceutical applications

A green organic-solvent-free route to prepare nanostructured zinc oxide carriers of clotrimazole for pharmaceutical applications.

Abstract

In the context of proposing cleaner production strategies for the pharmaceutical industry, an organic-solvent-free route to prepare nanostructured zinc oxide (NsZnO) reservoirs of clotrimazole (CTZ) was studied.

Two different NsZnO materials were synthesized, selecting wet chemical approaches without any organic solvents: chemical bath deposition and a soft-template sol-gel method. Both materials showed a pure crystalline wurzite structure with two different morphologies: aggregates of nanosheets or interconnected nanoparticles. For the former material the specific surface area and the pore volume reached the values of 66 m^2 /g and 0,230 cm^3 /g, respectively, which were higher than those of the latter (19 m^2 /g and 0,050 cm^3 /g).

For the first time, the loading of CTZ in a ZnO carrier was performed using supercritical CO_2 as a solvent. The NsZnO materials were characterized, before and after the drug loading, by FESEM, EDS, XRD, nitrogen adsorption isotherms, TGA, DSC, CTZ was dispersed in the NsZnO carrier in amorphous form, with a maximum loading of 17 % w/w. The decrease of specific surface area and pore volume upon drug loading for both samples is ascribed to the adsorption of CTZ molecules on the surface of the NsZnO materials. This confirms the feasibility of using the NsZnO as a CTZ carrier. In vitro drug-release was investigated and revealed that the NsZnO carrier can deliver CTZ with a faster release of a larger drug amount when compared to the solid crystalline drug.

The novel clean preparation route of a ZnO carrier for CTZ delivery herein presented is easily adabtable to batch small-scale pharmaceutical industrial process.

KEYWORDS

Zinc oxide, supercritical CO_2, drug loading, clotrimazole, drug-delivery.

1. **Introduction**

Nowadays the huge consumption of organic solvents by the pharmaceutical industries is becoming a well-known issue (Grodowska and Parczewski, 2010) and each year a high amount of waste is produced (Amado Alviz and Alvarez, 2016).

Two main issues derive from the use of organic solvents in pharmaceutical technologies: (i) the toxicity of residual solvents in the final products and (ii) the environmental impact (Amado Alviz and Alvarez, 2016). Therefore, in the last years even Life Cycle Assessment, which has been traditionally reserved to large scale continuous chemical and petrolchemical processes, has started to be applied to small scale batch pharmaceutical processes (Brunet et al., 2014).

The synthesis of Active Pharmaceutical Ingredients (APIs) is commonly considered the main step in which organic solvents are employed. Nevertheless, other sources of organic solvent wastes occur in the production of drug delivery systems, such as the synthesis of the carrier and the API loading (Li et al., 2013). Green and sustainable chemical processes are then highly desired to develop organic-solvent-free production of drug-delivery devices.

Though different studies have been reported regarding innovative greener approaches to load many API molecules into a wide amount of carriers (Li et al., 2013), scarce research has been focused on new organic-solvent-free routes for the loading of Clotrimazole (CTZ), a broad-spectrum antifungal drug. In the last decade, the use of CTZ in the pharmaceutical field has become increasingly important, due to its broad range of antimycotic activity. For this reason the development of new approaches to formulate and deliver CTZ is playing a key role (Crowley and Gallagher, 2014). Since the most significant limitation in the CTZ utilization is represented by its low water solubility, CTZ is often used in association with a wide range of organic solvents, which are generally employed during the drug loading step of pharmaceutical delivery systems. It is worth noting and somehow alarming that dangerous solvents, such as methanol (Jøraholmen et al., 2014)

and chloroform (Rai and Ravikumar, 2016; Verma and Ahuja, 2015), are still considered in the CTZ loading step for the development of new delivery systems. According to the "ICH guideline Q3C (R6) on impurities: guideline for residual solvents", which has been emended by the European Medicines Agency ("ICH Q3C Guideline, Impurities: Residual solvents.," 2016), both chloroform and methanol are solvents that should be limited in the pharmaceutical products because of their inherent toxicity (class 2 of this classification). Moreover, methanol has also been classified as one of the top four solvents used in the pharmaceutical sector with a dangerous impact on the environment and on health (Amado Alviz and Alvarez, 2016).

In the last decade, supercritical fluid technology has been emerging as an alternative to conventional drug loading techniques, such as the adsorption or impregnation from an organic solvent solution (Girotra et al., 2012). Supercritical carbon dioxide ($scCO_2$) is the most used supercritical solvent because of its unique chemical and physical properties. Since the compressibility of a supercritical fluid is high, the physical properties of $scCO_2$ can be easily tuned over a wide range with a minimal change in temperature or pressure. This is particularly significant as far as the density of the fluid is concerned because this property is strongly related to the solvent power. Eventually since the CO_2 is gaseous at ambient conditions, it simplifies the problem of solvent residues.

For the above-cited reasons, the $scCO_2$ is commonly considered the ideal substitute of many organic solvents in pharmaceutical applications (Pasquali and Bettini, 2008) and was proposed to achieve drug incorporation for several carriers. For example, the drug loading of polymers through $scCO_2$ assisted impregnation was widely reviewed (Champeau et al., 2015). Furthermore also the use of the $scCO_2$ in the preparation of drug-cyclodextrin inclusion complexes has already been investigated (Banchero et al., 2013),(Ravi et al., 2015).

As fas as zinc oxide is concerned, this is a widely known material which is traditionally used in several fields such as electronics (Kelly et al., 2016), optoelectronics, ceramic industry, nanotechnology and biomedicine (Kołodziejczak-Radzimska and Jesionowski, 2014). The general

aim of this work is to develop a green organic-solvent-free route to prepare ZnO-based drug carriers. ZnO was selected due to its intrinsic biological properties and its well-established use in dermatological and cosmetic products (Kołodziejczak-Radzimska and Jesionowski, 2014). Due to its low toxicity and high biocompatibility, ZnO has also been listed as a safe substance by Food and Drug Administration (21CFR182.8991).

A large variety of methods were reported in the literature for the production of ZnO nanostructures with particles differing in shape, size and spatial structure (Kołodziejczak-Radzimska and Jesionowski, 2014). However these methods result in many drawbacks, which include the use of toxic solvents, generation of hazardous by-products and the imperfection of the surface structure.

To the best of our knowledge the loading of drugs on NsZnO by means of $scCO_2$ has not been reported yet. In order to fill this gap, the main objective of this work has been the development of an innovative organic-solvent-free process which combines both the production of the NsZnO carrier and the drug loading phase of the API, i. e. the CTZ. Two NsZnO materials with different morphologies were synthesized using wet organic-solvent-free processes and they were characterized to elucidate their morphological and physico-chemical properties. A $scCO_2$ drug loading technique was used to load the CTZ on the NsZnO so allowing the final material to be recovered without any solvent residue. Moreover preliminary *in vitro* dissolution studies were performed to verify the capability of the obtained materials to release the CTZ in view of future drug delivery applications.

Eventually it must be pointed that, in the perspective of the industrial development of the supercritical fluid technology (Perrut et al., 2000), the preparation route here proposed can be easily transferred to real pharmaceutical industry, which traditionally involves small-scale batch processes. However**,** the limitation of the present study is the lack of in vitro studies mimicking the biological environment and conditions envisaged for the applications of these systems, which will be investigated in future work.

2. Materials and Methods

Zinc Chloride ($ZnCl_2$), zinc acetate ($Zn(CH_3CO_2)_2$), non-ionic poly-(ethyleneoxide)-poly(propyleneoxide)-poly(ethyleneoxide) amphiphilic triblock copolymer (Pluronic F127), urea (NH_2CONH_2), hydrochloric acid (HCl) (37%) and clotrimazole ($C_{22}H_{17}ClN_2$) were purchased from Sigma–Aldrich and used as received. Carbon dioxide with a purity of 99.998% was supplied by SIAD (Italy). Bidistilled water was used throughout this study.

2.1 Synthesis of nanostructured ZnO

Two different NsZnO materials were synthesized. For this purpose two wet chemical processes without any organic solvent were selected: chemical bath deposition and a soft-template sol-gel method.

2.1.1 Chemical bath deposition

The key mechanism of the chemical bath deposition (CBD) approach is based on the growth of layered inorganic materials, which contain Zn^{2+} ions, as precursors of ZnO. Many CBD processes that employ basic aqueous solvents and zinc salts for the fabrication of ZnO nanostructures have been reported in the literature due to several advantages, such as the easiness in preparation, cheap equipment, low deposition temperature (< 100 °C) and versatility (Kawano and Imai, 2010; Khayatian et al., 2016; Koao et al., 2014; Shaikh et al., 2016; Shi et al., 2015).

The CBD procedure here investigated was previously described by Kakiuchi and co-workers (Kakiuchi et al., 2006). $ZnCl_2$ and urea were used as starting reagents in order to obtain zinc carbonate hydroxide hydrate ($Zn_4CO_3(OH)\cdot 6H2O$) with a nanosheet-like morphology, which is the precursor of ZnO. However some changes have been here introduced in the recovery of the ZnO precursor before calcination.

Zinc chloride and urea were dissolved in bidistilled water in order to achieve a final concentration of 0.05 M of Zn^{2+} and 1.0 M of urea. The pH value of the solution was adjusted to 4 by using hydrochloric acid. At the end of these preliminary operation steps a transparent and precipitate-free

solution was obtained. The solution was kept under magnetic stirring at 80°C for 24 hours using the reflux technique until the deposition of a white dense precipitate of $Zn_4CO_3(OH)_6 \cdot H_2O$ was obtained. The suspension with the nanosheet-shaped ZnO precursor was carefully filtered allowing the precipitate to be separated on the surface of a cellulose filter (Whatman® qualitative filter paper, Grade 3): a powder was then obtained instead of a film. Finally the precipitate was thermally treated by heating it at 300°C for 0.5 hour in a static oven to be transformed into zinc oxide. In the following sections the material obtained with the above described procedure is referred as NsZnO-1.

2.1.2 Soft-template sol-gel method

The use of a soft template in the synthesis of NsZnO materials has been scarcely investigated in the literature. Zinc acetate was selected as the zinc source and Pluronic F127 as the templating agent. A solution of Pluronic F127 (10% v/v) in water was prepared. Zinc acetate was then added until a concentration equal to 0.8 M was obtained. An opalescent suspension was immediately formed and was left under magnetic stirring at room temperature for 2 hours. Finally the suspension was dried under vacuum and the dried residue was calcinated at 500°C for about 2 hours and 45 minutes with a heating rate of 3°C/min in order to remove the template and obtain zinc oxide. In the following sections the material obtained with the above described procedure is referred as NsZnO-2.

2.2 Drug loading through supercritical carbon dioxide

The supercritical impregnation process was carried out by contacting the drug and each of the two NsZnO materials in a static atmosphere of $scCO_2$ at constant temperature and pressure. The apparatus and the experimental procedure adopted to achieve the incorporation of the drug into the NsZnO are described in a previous work (Banchero et al., 2009). A tailored set-up, which was already used in a previous work (Gignone et al., 2014), was applied to place the samples inside the supercritical impregnation vessel. First a pellet of the drug (100 mg) and a pellet of the NsZnO (100 mg) were prepared and introduced into a glass cylinder of 1 cm diameter. A disc of filter paper was

placed between the two pellets to prevent their contact and guarantee an efficient recovery of the samples at the end of the drug loading process (Figure 1). Both the NsZnO and the drug were accurately pelletized using a manual hydraulic press to obtain small cylindrical pellets with a 9 mm diameter and a height ranging from 1 to 2 mm. Each glass device was supposed to contain one single combination of a NsZnO pellet and a drug pellet.

The sample-loaded glass devices were placed inside a stainless steel vessel, which was put in an oven that kept all the system at constant temperature. To assure reproducibility the vessel can hold up to 5 homemade glass cylinders and this endows different batches of the same sample to be obtained at the end of the impregnation process.

Liquid CO_2 was used to fill the vessel, then the temperature was increased to 100°C and additional CO_2 was pumped to reach the target pressure (25.0 MPa): these operative conditions did not not affect the CTZ stability (Hoogerheide and Wyka, 1982). The system was maintained at the above-reported conditions for several hours (around 12) to allow the drug to be dissolved in the $scCO_2$ and diffuse into the NsZnO.

At the end of the drug loading process, the apparatus was brought back to atmospheric pressure and cooled to room temperature.

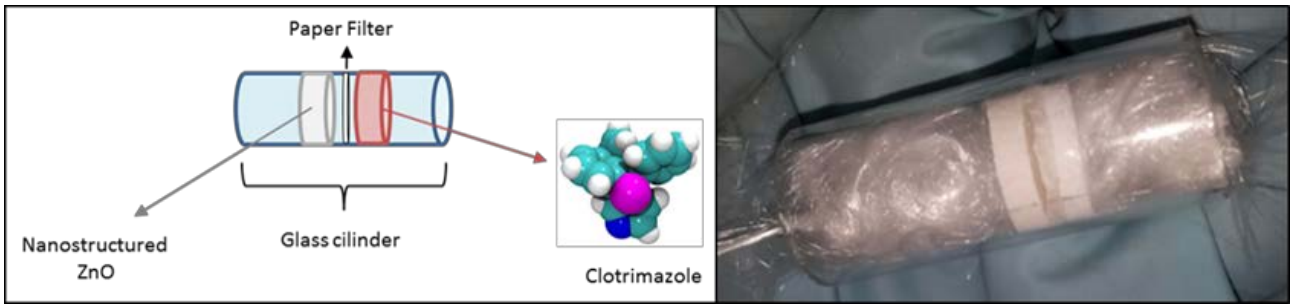

Figure 1 Schematic representation of the homemade device used to perform the incorporation of the drug by means of $scCO_2$ (left side); picture showing the filled glass cylinder, ready for the incorporation process (right side).

3. Experimental

3.1 Characterization

The physico-chemical characterization of the NsZnO samples was performed by means of X-ray diffraction (XRD), thermogravimetry (TG), differential scanning calorimetry (DSC), nitrogen adsorption isotherms, and field emission scanning microscopy (FESEM) coupled with EDS.

XRD patterns were obtained using a PANalytical X'Pert (Cu Kα radiation) diffractometer. Data were collected with a 2D solid state detector (PIXcel) from 20 to 70 2θ with a step size of 0.001 2θ and a wavelength of 1.54187 Å. Crystallites size was determined according to Scherrer equation (Scherrer, 1918) by comparing the profile width of a standard profile with the sample profile. The Scherrer equation relates the width of a powder diffraction peak to the average dimensions of crystallites in a polycrystalline powder:

$$D = K\lambda / \beta_{(2\theta)hkl} \cos\theta$$

where β is the crystallite size contribution to the peak width (full width at half maximum) in radians, K (shape factor) is a constant near unit and D is the average thickness of the crystal in a direction normal to the diffracting plane hkl.

Profile fits were performed using X'Pert High Score Plus, using Pseudo-Voigt peak function with Kα1 and Kα2 fitting on a background stripped pattern. The sample-induced peak broadening β was determined by subtracting the instrumental peak width from the measured peak width.

The instrumental broadening was determined using LaB6 powder (NIST SRM®660a, size of crystallites in the 2 μm to 5 μm range).

TG analyses were carried out between 20°C and 800°C in air (flow rate 100 mL/min with a heating rate of 10 °C /min) using a SETARAM 92 instrument while the DSC measurements were performed under nitrogen flux (60 ml/min), in the range between 50° C and 200° C, with a DSCQ 1000 by TA Instrument.

Nitrogen adsorption isotherms were measured using a Quantachrome AUTOSORB-1 instrument. Before the adsorption measurements, samples were outgassed for 2 h at 100° C. BET specific surface areas (SSA_{BET}) were calculated in the relative pressure range of 0.04–0.1.

FESEM images were recorded with a FESEM ZEISS MERLIN instrument, equipped with an EDS detector (OXFORD).

For the measurement of CTZ concentration in the release tests a UV-Vis Beckman-Coulter spectrophotometer was used.

3.2 Preliminary in vitro drug release study

A preliminary in vitro release study was performed to assess the ability of the drug-loaded NsZnO to release the drug. Multicompartment rotating cells, equipped with a hydrophilic dialysis membrane (Spectra/Por, Spectrum®, cut-off 12000-14000 Da), were used to perform the in vitro release tests. The release profiles of CTZ-loaded NsZnO-1 sample was compared with that of pure crystalline CTZ. A HCl 0.1 M solution was used as the receiving phase (Szymanska and Winnicka, 2013). After fixed time intervals, the receiving phase was completely replaced by a fresh solution. The release study took approximately 2 hours. A quantitative analysis by UV spectroscopy at 254 nm was carried out in order to determine the amount of released drug on each withdrawn sample.

4. Results and Discussion

4.1 Characterization of the NsZnO materials as such.

Figure 2 reports the FESEM images, at low and high magnification, of the NsZnO-1 sample. NsZnO-1 appears as aggregates of nanosheets with thickness of about 20 nm that are formed by the self-assembling of ovoid nanoparticles (around 15-20 nm). This morphology is in agreement with the mechanism growth proposed by Kakiuchi et al. (Kakiuchi et al., 2006).

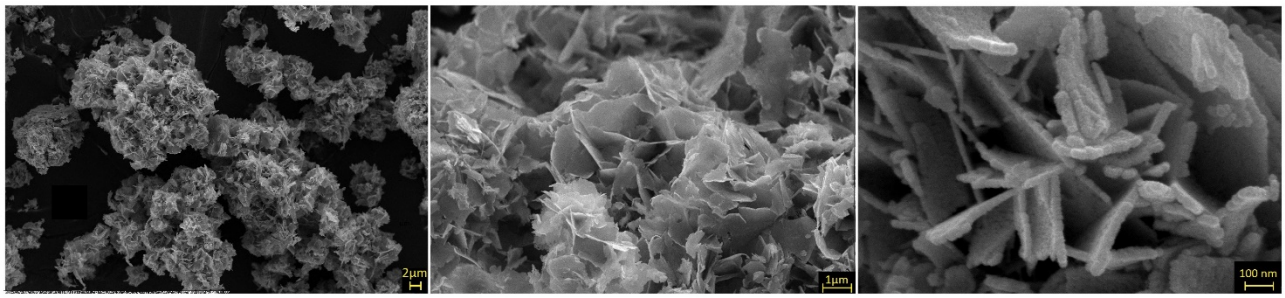

Figure 2 FESEM images of NsZnO-1 (magnification: 5.00 K X, 25.00 K X, 250.00 K X)

The morphology of NsZnO-2 is visible in Figure 3 at different magnification. The material appears in form of micrometric and sub-micrometric aggregates of interconnected nanoparticles with heterogeneous size of tens nanometers.

The presence of the nanometric particles might be explained considering a mechanism where the Pluronic F127 molecules would restrict the growth of the ZnO precursor (Ueno et al., 2013).

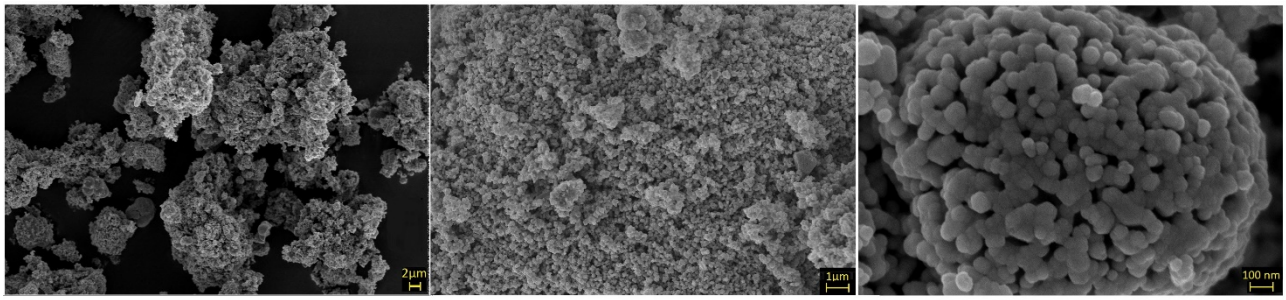

Figure 3 FESEM images of NsZnO-2 (magnification: 5.00 K X, 25.00 K X, 250.00 K X)

EDS analysis (Supplementary Information) confirm the presence of Zn and O at the surface in both samples. No occurrence of chloride is observed for NsZnO-1, from which the complete transformation of the $ZnCl_2$ precursor can be inferred.

Figure 4 reports the XRD patterns of both NsZnO materials, which reveal the occurrence of a highly crystalline single hexagonal phase of wurtzite structure. The five main reflection peaks (100), (002), (101), (102) and (110) and the intensity distribution of the peaks are consistent with those of the standard card for the hexagonal phase ZnO (JCPDS ICDD 36-1451). In both the XRD

patterns reported in Figure 4 the characteristic peaks of the precursors cannot be detected: this means that pure ZnO can be obtained through the above-described synthetic methods. Comparing the XRD patterns of the two samples, it is evident that NsZnO-1 shows broader peaks than NsZnO-2.

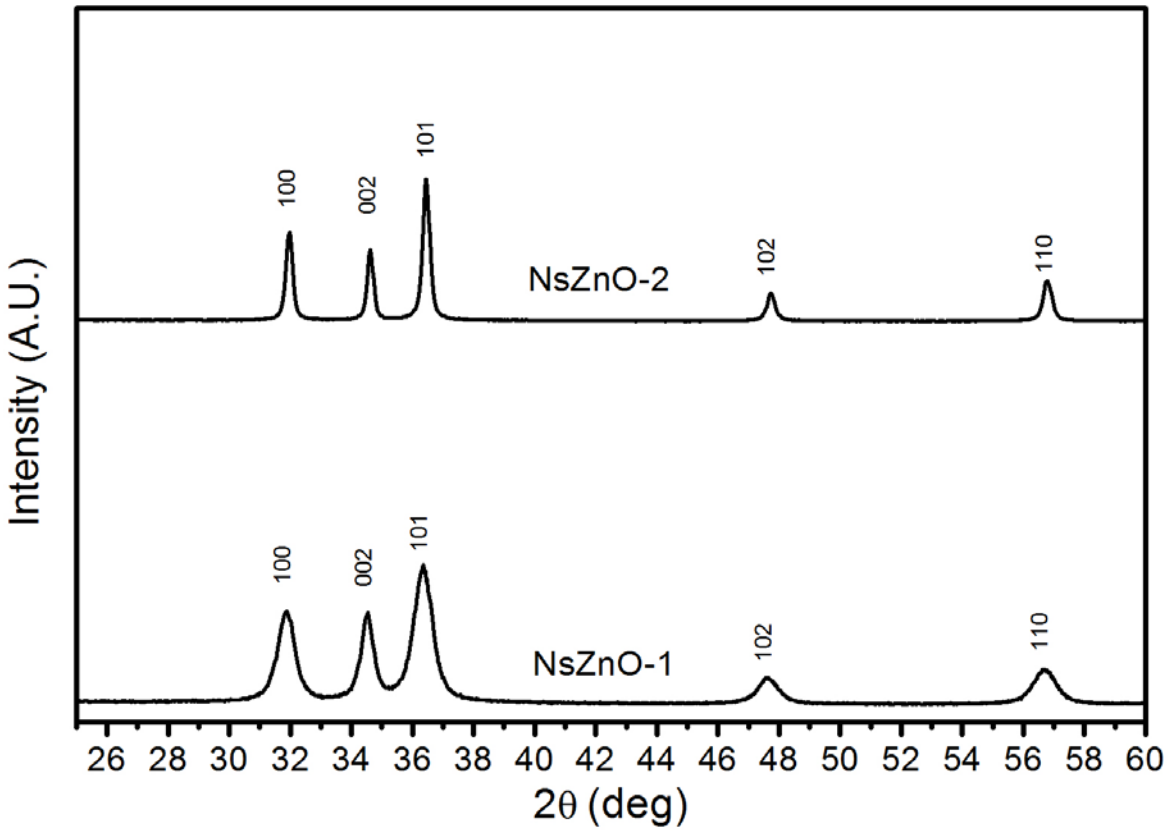

Figure 4 XRD patterns of NsZnO-1 e NsZnO-2

N_2 physisorption measurements were used to evaluate the specific surface area (m^2/g) and the pore volume (m^3/g) of the two samples. NsZnO-1 shows values of both parameters higher than those of NsZnO-2 (Table 1). These results are in agreement with the smaller particles size revealed for the former sample by FESEM and XRD data.

4.2 Characterization of the CTZ-loaded NsZnO materials

$ScCO_2$ was used to load CTZ inside the two NsZnO materials, TG analyses of the NsZnO materials loaded with CTZ (CZT@NsZnO) allowed the amount of CTZ to be evaluated, which corresponds to 17% w/w for CZT@NsZnO-1 and 14% w/w for CZT@NsZnO-2, respectively (Table 1).

Table 1 Surface area and pore volume values before and after the CTZ loading, together with the amount of CTZ adsorbed into NsZnO materials by $scCO_2$ process

	Before drug incorporation		***After drug incorporation***		***Amount of CTZ incorporated***
	Surface Area ***(m^2/g)***	***Pore Volume*** ***(cm^3/g)***	***Surface Area*** ***(m^2/g)***	***Pore Volume*** ***(cm^3/g)***	***W/W %***
NsZnO-1	66	0,230	22	0,110	17
NsZnO-2	19	0,050	6,7	0,003	14

Figure 5 shows the isotherms of both the NsZnO materials before and after the loading of CTZ through $scCO_2$. The values of the surface area and pore volume values are reported in Table 2.

As far as NsZnO-1 is concerned, the BET specific surface area decreased from 66 m^2/g, for the as-synthetized material, to 22 m^2/g, after CTZ loading, whereas the pore volume decreased from 0.230 cm^3/g to 0.110 cm^3/g. The BET specific surface area of NsZnO-2, instead, decreased from 19 m^2/g to 6.7 m^2/g and the pore volume decreased from 0.050 cm^3/g to 0.003 cm^3/g.

The BET specific surface area of NsZnO-1 is lower than the value reported in literature for the nanostructured ZnO deposited in the film form on a glass substrate (88.5 m^2/g) (Kakiuchi et al., 2006) As far as the sample NsZNO-2 is concerned, no comparison with the value reported in literature is possible because of the lack of this datum (Ueno et al., 2013).

The decrease of BET specific surface area and pore volume upon CTZ loading for both samples is ascribed to the adsorption of CTZ molecules on the surface of NsZnO materials. This confirms the feasibility of using the NsZnO as CTZ carrier.

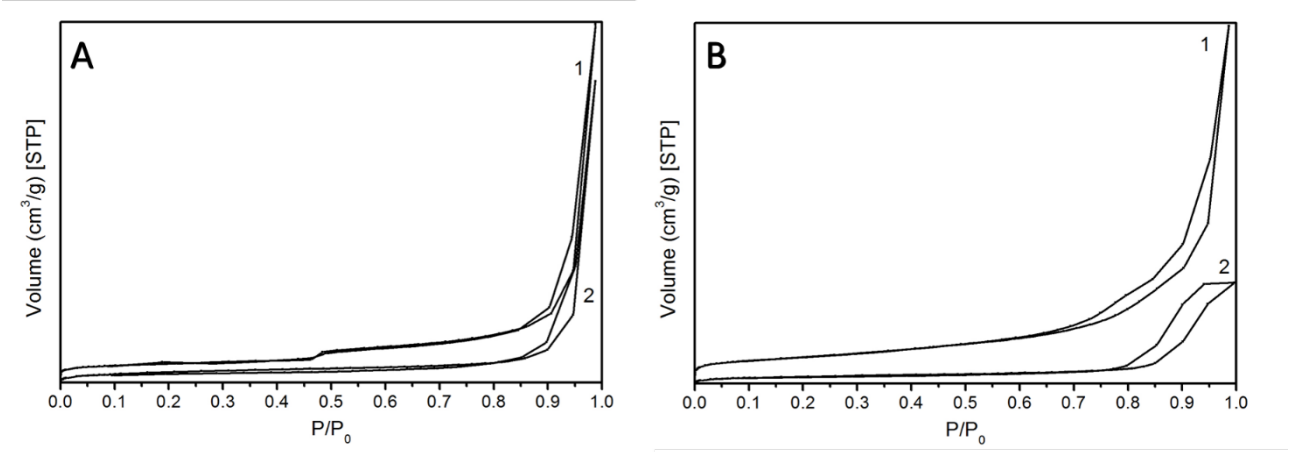

Figure 5 Section A: N_2 adsorption-desorption isotherms of NsZnO-1 before (1) and after (2) CTZ loading. Section B: N_2 adsorption-desorption isotherms of NsZnO-2 before (1) and after (2) CTZ loading

XRD and DSC analyses were performed to investigate the form of the drug inside the NsZnO materials pores. Figure 6 reports the XRD patterns of CTZ@NsZnO-1 and CTZ@NsZnO-2. Both materials show the typical hexagona wurtzite structure. The crystallites size determined using the Scherrer equation (not reported) are similar to values reported in Table 2.

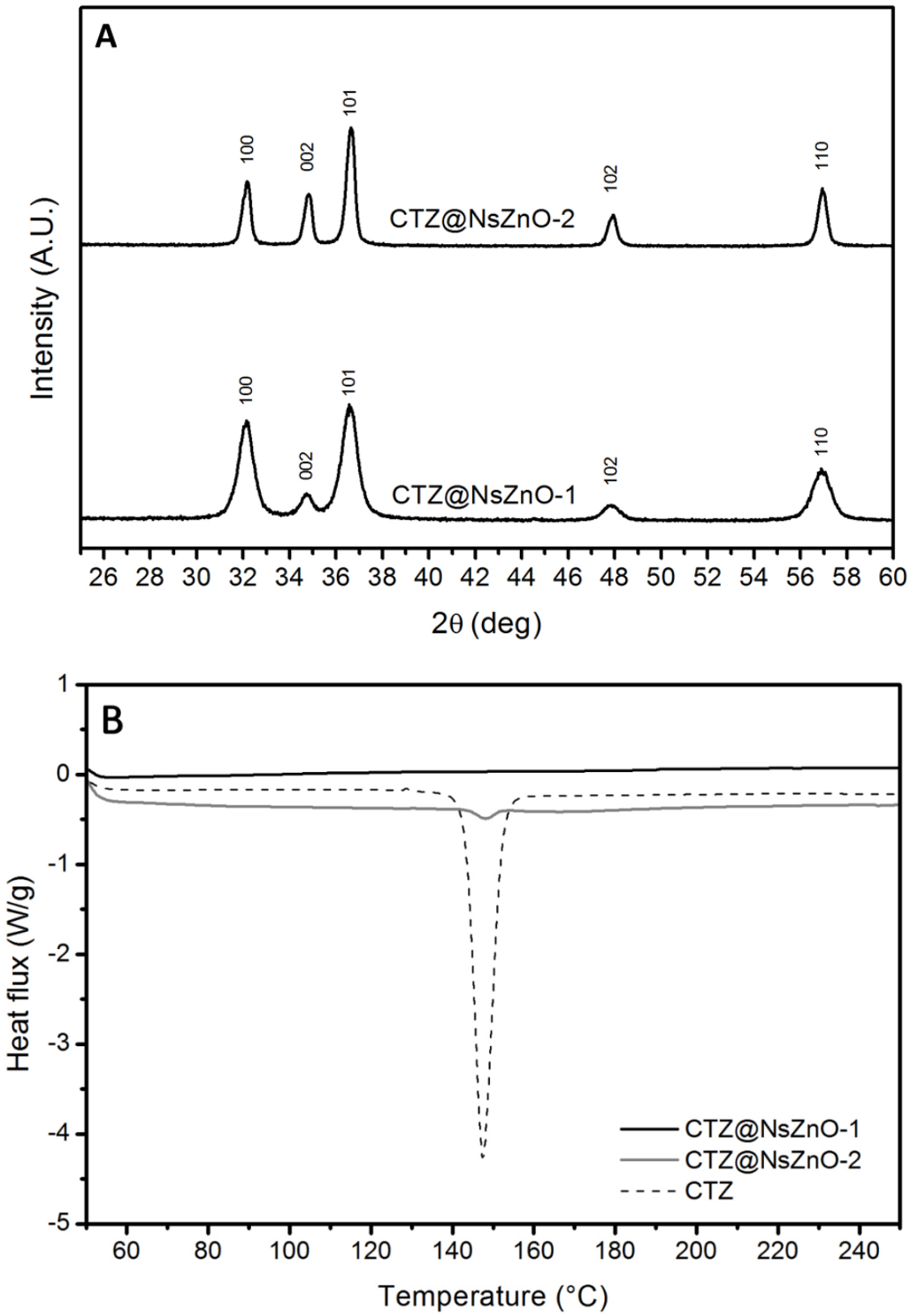

Figure 6 XRD patterns and DSC analyses of CTZ-loaded NsZnO materials after $scCO_2$ impregnation process. Figure 6A shows the XRD patterns of CTZ@NsZnO-1 and CTZ@NsZnO-2. Figure 6B reports the DSC curves of pure crystalline CTZ, CTZ@NsZnO-1 and CTZ@NsZnO-2.

Table 2 Crystallite dimensions (nm) determined from application of the Scherrer equation to selected hkl reflections of NsZnO-1 and NsZnO-2

hkl	***NsZnO-1***	***NsZnO-2***
100	15	38
101	15	33
102	16	24
110	14	24

No additional diffraction peaks of the crystalline CTZ are observed in both cases. This evidences that the loaded drug molecules are not assembled in the crystalline structure. The same result was also confirmed by the DSC analysis. DSC curves for pure CTZ, CTZ@NsZnO-1 and CTZ@NsZnO-2 are shown in Figure 6B. Pure CTZ showed a sharp melting endotherm peak at 147 °C, in agreement with what reported in the product data sheet. No evidence of this peak was observed in the DSC curve of CTZ@NsZnO-1 (curve A), suggesting a complete amorphization of the drug in the carrier. The DSC curve of CTZ@NsZnO-2 (curve B) showed a dramatic decrease in the intensity of the drug melting peak, being only a very weak signal discernible. The disappearance or decrease in intensity of the drug endothermic peak is generally related to drug–material interactions and/or loss of drug crystallinity.

The presence of a residual weak melting endotherm peak in the case of CTZ@NsZnO-2 is in agreement with the lower SSA (19 m^2/g) with respect to CTZ@NsZnO-1 (66 m^2/g). In fact, despite the higher amount of loaded CTZ in the latter sample (17 % w/w), complete amorphization is ascribed to the interaction between the drug molecules and the ZnO surface.

From the content of CTZ (% w/w) the number of molecules of CTZ per gram of ZnO was evaluated and, using the SSA value, this was transformed into the number of molecules per nm^2, which resulted to be equal to 5.4 for NsZnO-1.

The significantly lower SSA value of NsZnO-2 accounts for its lower capacity to form CTZ-surface interactions, favouring partial CTZ self-aggregation in crystalline form. Indeed, the amount of molecules/nm^2 in CTZ@NsZnO-2 resulted to be equal to 15.

4.3 Preliminary in vitro drug release study

Previous results showed the possibility to load CTZ molecules into NsZnO materials by means of $scCO_2$. The capability of releasing the loaded CTZ was also investigated. For this purpose an in vitro release study of CTZ from NsZnO-1, i. e. the sample showing the higher CTZ content in amorphous form, was carried out using a multi-compartmental rotating cell.

Figure 7 reports the cumulative percentage release curves of CTZ both from CTZ@NsZnO-1 and unsupported pure CTZ.

The release profile of CTZ from CTZ@NsZnO-1 shows a fast release in the first 10 minutes of the test, where the amount of CTZ released by CTZ@NsZnO-1 was about 15 μg. Then the quantity of released drug kept slightly increasing over time until it was approximately doubled. This trend was significantly different from the release profile of unsupported CTZ. In fact in this case the quantity released after 10 minutes was less than the half of that released by CTZ@NsZnO in the same time. At the end of experiment, the final quantity of released CTZ was about 25 % of that released by CTZ@NsZnO-1.

These results show that CTZ is not irreversibly confined in the NsZnO material and that NsZnO can act as a drug delivery carrier, ensuring a fast release of a larger CTZ amount in comparison with the unsupported crystalline drug. This might play a key role in several biological applications where the bioavailability of poorly-water-soluble drugs is still a challenging issue.

A possible explanation of this behaviour is the amorphous nature of CTZ hosted in the NsZnO sample. Amorphization of drugs on carriers has been already reported in literature. Several matrices were investigated such as mesoporous silica (Gignone et al., 2015, 2014; McCarthy et al., 2016), cyclodextrins (Al-Marzouqi et al., 2009; Banchero et al., 2013; Hussein et al., 2007; Ravi et al.,

2015) and polymers (Banchero et al., 2009). It is widely accepted that the amorphization of the drug molecules plays a key role in increasing their dissolution rate and solubility, which are two fundamental parameters that affect the subministration of poorly-water-soluble active ingredients, such as CTZ.

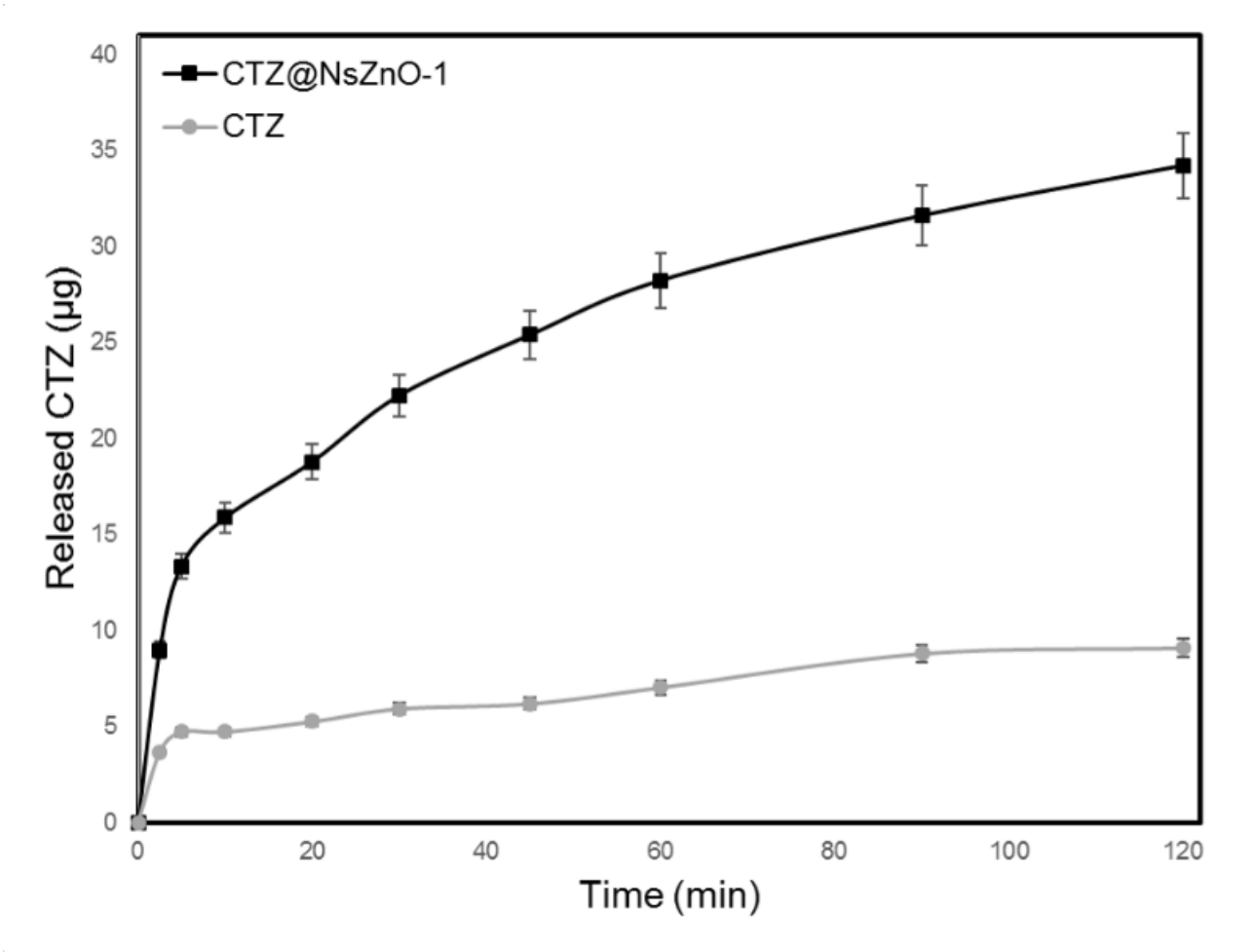

Figure 7 In vitro drug-release profiles of clotrimazole from pure crystalline clotrimazole and CTZ@NsZnO-1

5. Conclusions

An organic-solvent-free route to obtain a NsZnO reservoir of CTZ was studied.

Two NsZnO materials with the hexagonal wurtzite structure and different morphologies were synthesized using wet organic-solvent-free processes. In particular, existing approaches reported in

the literature for the synthesis of nanostructured ZnO films or nanosheets were properly modified to prepare novel NsZnO particles.

CTZ was loaded into NsZnO through $scCO_2$ impregnation and, at the best of our knowledge, this is the first time that a technology employing supercritical carbon dioxide was used for the drug loading of ZnO-based carriers, in order to obtain ready-to-use drug loaded materials.

The physico-chemical characterization of NsZnO before and after the loading of CTZ revealed that the $scCO_2$ process does not significantly affect the structure of the materials. The CTZ loading for the two NsZnO materials was equal to 14 %w/w and 17 % w/w, respectively. XRD and DSC analysis revealed that CTZ is distributed in the NsZnO carrier in amorphous form.

The release profiles of CTZ in a HCl 0.1 M solution was investigated. Results revealed that CTZ is not irreversibly confined in the NsZnO support and that NsZnO can act as a drug delivery carrier, which ensures a faster release and a larger drug amount than that of the solid crystalline drug. This might play a key role in several biological applications where the bioavailability of poorly-water-soluble drugs is still a challenging issue.

The reported results support the idea that the novel production routes here proposed to obtain NsZnO drug delivery carriers for CTZ are feasible and can be a promising solvent-free alternative to the conventional ones since they are easily adabtable to batch small-scale pharmaceutical industrial process.

Acknowledgments

This study was supported by the MIUR PhD grant financial funding. Special thanks are due to Cristiano Bugnone from Politecnico di Torino for his kind collaboration.

References

Al-Marzouqi, A.H., Elwy, H.M., Shehadi, I., Adem, A., 2009. Physicochemical properties of antifungal drug-cyclodextrin complexes prepared by supercritical carbon dioxide and by conventional techniques. J. Pharm. Biomed. Anal. 49, 227–233. doi:10.1016/j.jpba.2008.10.032

Amado Alviz, P.L., Alvarez, A.J., 2016. Comparative life cycle assessment of the use of an ionic liquid ([Bmim]Br) versus a volatile organic solvent in the production of acetylsalicylic acid. J. Clean. Prod. doi:10.1016/j.jclepro.2017.02.107

Banchero, M., Manna, L., Ronchetti, S., Campanelli, P., Ferri, A., 2009. Supercritical solvent impregnation of piroxicam on PVP at various polymer molecular weights. J. Supercrit. Fluids 49, 271–278. doi:10.1016/j.supflu.2009.01.008

Banchero, M., Ronchetti, S., Manna, L., 2013. Characterization of Ketoprofen / Methyl-Beta-Cyclodextrin Complexes Prepared Using Supercritical Carbon Dioxide. J. Chem. 2013, 8. doi:10.1155/2013/583952

Brunet, R., Guillén-Gosálbez, G., Jiménez, L., 2014. Combined simulation-optimization methodology to reduce the environmental impact of pharmaceutical processes: Application to the production of Penicillin v. J. Clean. Prod. 76, 55–63. doi:10.1016/j.jclepro.2014.02.012

Champeau, M., Thomassin, J., Tassaing, T., Jérôme, C., 2015. Drug loading of polymer implants by supercritical CO 2 assisted impregnation : A review. J. Control. Release 209, 248–259. doi:10.1016/j.jconrel.2015.05.002

Crowley, P.D., Gallagher, H.C., 2014. Clotrimazole as a pharmaceutical: past, present and future. J. Appl. Microbiol. 117, 611–617. doi:10.1111/jam.12554

Gignone, A., Manna, L., Ronchetti, S., Banchero, M., Onida, B., 2014. Microporous and Mesoporous Materials Incorporation of clotrimazole in Ordered Mesoporous Silica by supercritical CO 2. Microporous Mesoporous Mater. 200, 291–296. doi:10.1016/j.micromeso.2014.05.031

Gignone, A., Piane, M.D., Corno, M., Ugliengo, P., Onida, B., 2015. Simulation and Experiment Reveal a Complex Scenario for the Adsorption of an Antifungal Drug in Ordered Mesoporous Silica. J. Phys. Chem. C 119, 13068−13079. doi:10.1021/acs.jpcc.5b02666

Girotra, P., Singh, S.K., Nagpal, K., 2012. Supercritical fluid technology : a promising approach in pharmaceutical research. Pharm. Dev. Technol. 18, 22–38. doi:10.3109/10837450.2012.726998

Grodowska, K., Parczewski, a., 2010. Organic solvents in the pharmaceutical industry. Acta Pol. Pharm. 67, 3–12. doi:10.1021/cg034055z

Hoogerheide, J.G., Wyka, B.E., 1982. Clotrimazole. Anal. Profiles Drug Subst. 11, 225–255. doi:10.1016/S0099-5428(08)60265-8

Hussein, K., Türk, M., Wahl, M.A., 2007. Comparative evaluation of ibuprofen/β-cyclodextrin complexes obtained by supercritical carbon dioxide and other conventional methods. Pharm. Res. 24, 585–592. doi:10.1007/s11095-006-9177-0

ICH Q3C Guideline, Impurities: Residual solvents. [WWW Document], 2016. URL https://www.ich.org/fileadmin/Public_Web_Site/ICH_Products/Guidelines/Quality/Q3C/Q3C_R6__Step_4.pdf (accessed 6.26.17).

Jøraholmen, M.W., Vanić, Ž., Tho, I., Škalko-Basnet, N., 2014. Chitosan-coated liposomes for topical vaginal therapy: Assuring localized drug effect. Int. J. Pharm. 472. doi:10.1016/j.ijpharm.2014.06.016

Kakiuchi, K., Hosono, E., Kimura, T., Imai, H., Fujihara, S., 2006. Fabrication of mesoporous ZnO nanosheets from precursor templates grown in aqueous solutions. J. Sol-Gel Sci. Technol. 39, 63–72. doi:10.1007/s10971-006-6321-6

Kawano, T., Imai, H., 2010. Nanoscale morphological design of ZnO crystals grown in aqueous solutions. J. Ceram. Soc. Japan 118, 969–976.

Kelly, L.L., Racke, D.A., Kim, H., Ndione, P., Sigdel, A.K., Berry, J.J., Graham, S., Nordlund, D., Monti, O.L.A., 2016. Hybridization-Induced Carrier Localization at the C60/ZnO Interface.

Adv. Mater. 28, 3960–3965. doi:10.1002/adma.201503694

Khayatian, A., Kashi, M.A., Azimirad, R., Safa, S., Akhtarian, S.F.A., 2016. Effect of annealing process in tuning of defects in ZnO nanorods and their application in UV photodetectors. Opt. - Int. J. Light Electron Opt. 127, 4675–4681. doi:10.1016/j.ijleo.2016.01.177

Koao, L.F., Dejene, F.B., Swart, H.C., 2014. Properties of flower-like ZnO nanostructures synthesized using the chemical bath deposition. Mater. Sci. Semicond. Process. 27, 33–40. doi:10.1016/j.mssp.2014.06.009

Kołodziejczak-Radzimska, A., Jesionowski, T., 2014. Zinc Oxide—From Synthesis to Application: A Review. Materials (Basel). 7, 2833–2881. doi:10.3390/ma7042833

Li, M., Lv, S., Tang, Z., Song, W., Yu, H., Sun, H., Liu, H., Chen, X., 2013. Polypeptide/Doxorubicin Hydrochloride Polymersomes Prepared Through Organic Solvent-free Technique as a Smart Drug Delivery Platform. Macromol. Biosci. 13, 1150–1162. doi:10.1002/mabi.201300222

McCarthy, C.A., Ahern, R.J., Dontireddy, R., Ryan, K.B., Crean, A.M., 2016. Mesoporous silica formulation strategies for drug dissolution enhancement: a review. Expert Opin. Drug Deliv. 13, 93–108. doi:10.1517/17425247.2016.1100165

Pasquali, I., Bettini, R., 2008. Are pharmaceutics really going supercritical? Int. J. Pharm. 364, 176–187. doi:10.1016/j.ijpharm.2008.05.014

Rai, S.Y., Ravikumar, P., 2016. Development and evaluation of microsphere based topical formulation using design of experiments. Indian J. Pharm. Sci. 78. doi:10.4172/pharmaceutical-sciences.1000102

Ravi, S., Rudrangi, S., Trivedi, V., Mitchell, J.C., Wicks, S.R., Alexander, B.D., 2015. Preparation of olanzapine and methyl- b -cyclodextrin complexes using a single-step , organic solvent-free supercritical fl uid process : An approach to enhance the solubility and dissolution properties. Int. J. Pharm. 494, 408–416. doi:10.1016/j.ijpharm.2015.08.062

Scherrer, P., 1918. Bestimmung der Grösse und der inneren Struktur Internal, Kolloidteilchen

mittels Röntgensrahlen [Determination of the size and Goettingen, structure of colloidal particles using X-rays]. Nachr Ges Wiss Germa, Math-Phys Kl. 98–100.

Shaikh, S.K., Inamdar, S.I., Ganbavle, V. V., Rajpure, K.Y., 2016. Chemical bath deposited ZnO thin film based UV photoconductive detector. J. Alloys Compd. 664, 242–249. doi:10.1016/j.jallcom.2015.12.226

Shi, Y., Truong, V.X., Kulkarni, K., Qu, Y., Simon, G.P., Boyd, R.L., Perlmutter, P., Lithgow, T., Forsythe, J.S., 2015. Light-Triggered Release of Ciprofloxacin from an in situ Forming Click Hydrogel for Antibacterial Wound Dressings. J. Mater. Chem. B 3–6. doi:10.1039/C5TB01820J

Szymanska, E., Winnicka, K., 2013. Comparison of flow-through cell and paddle methods for testing vaginal tablets containing a poorly water-soluble drug. Trop. J. Pharm. Res. 12, 39–44. doi:Doi 10.4314/Tjpr.V12i1.7

Ueno, N., Dwijaya, B., Uchida, Y., Egashira, Y., Nishiyama, N., 2013. Synthesis of mesoporous ZnO, AZO, and BZO transparent conducting films using nonionic triblock copolymer as template. Mater. Lett. 100, 111–114. doi:10.1016/j.matlet.2013.03.011

Verma, P., Ahuja, M., 2015. Optimization, characterization and evaluation of chitosan-tailored cubic nanoparticles of clotrimazole. Int. J. Biol. Macromol. 73. doi:10.1016/j.ijbiomac.2014.10.065